Dependence of pedestal structure on collisionality in JT-60U

H. Urano[1], N. Aiba[2], K. Kamiya[1], Y. Kamada[1] and the JT-60 Team[1]
[1] *Japan Atomic Energy Agency, Naka, Ibaraki 311-0193 Japan*
[2] *Japan Atomic Energy Agency, Rokkasho, Aomori 039-3212, Japan*

1. Introduction

The characterisation of pedestal structure has intensively been addressed from the perspective of edge dimensionless parameters, aiming at the extrapolation towards ITER. It has been recognised that the spatial width in H-mode pedestal region depends strongly on the poloidal beta value as [1–4]:

$$\Delta_{\Psi_N} = \beta^{1/2} \cdot f\left(\nu^*, \kappa, \epsilon, \cdots\right) \tag{1}$$

where Δ_{Ψ_N} denotes the pedestal width in the normalized poloidal flux space. There is a strong correlation existing between β and ρ^* because of the constraint of ELMs. Thus, the dependence of pedestal width on β and ρ^* has mainly been studied at a given magnetic geometry in many tokamaks. In other words, the dependence of pedestal width on the other dimensionless parameters, such as ν^*, κ, ϵ, etc, has not been fully understood.

This paper reports the experimental result on the dependence of pedestal width on ν^* in JT-60U. In a metallic wall, high gas puff rate is necessary to have the screening effect to avoid high Z impurity influxes where the pedestal ν^* may be high. The characteristics of pedestal structure in high ν^* regime is also important. Thus, there are two ν^* scans conducted in ITER-relevant low ν^* regime ($0.03 \leq \nu^* \leq 0.2$) and high ν^* regime ($0.2 \leq \nu^* < 0.8$).

2. Experiments in ITER-relevant low ν^* regime

In ITER-relevant low ν^* regime, a dimensionless collisionality scan experiment has been conducted. The pure collisionality scan requires the experimental setup which satisfies the following conditions:

$$n \propto I_p^0, \quad T \propto I_p^2, \quad I_p \propto B_t \tag{2}$$

where n, T, I_p and B_t denote the density, temperature, plasma current and magnetic field, respectively. The other dimensionless parameters relevant to the magnetic geometry such as q, κ, ϵ, etc are fixed. These conditions lead to the experiment in which the plasma density remains constant with sufficient heating for satisfying $T \sim I_p^2$. Figs. 1(a) and (b) show the temporal evolution of plasma parameters at low and high ν^*, respectively. The I_p and B_t are 1.79 MA and 4.0 T in the low ν^* discharge whereas those are 1.03 MA and 2.3 T in the high ν^* discharge, so that q_{95} is ~ 3.9 for both cases. The plasma configuration is fixed at $R = 3.3$m, $a = 0.8$m, $\delta = 0.34$, $\kappa = 1.5$. The line-averaged electron density is also controlled at $\bar{n}_e \sim 2.8 \times 10^{19}\mathrm{m}^{-3}$. The scan ranges of I_p and B_t were chosen base on the experimental condition with practically controllable values of β_p and $\bar{n}_e/n_{GW}$.

Figs. 2(a) and (b) show the spatial profiles of n_e and T_i at two time slices indicated by a broken line in figure 1, respectively. The ν^* was varied by the factor of 5 from 0.04 to 0.19 whereas the other dimensionless parameters were almost fixed. The n_e profiles are approximately similar. Edge T_i profiles are self-similar and differ by the factor of ~ 4 with nearly the same pedestal width. However, the difference in the pedestal T_i is larger than

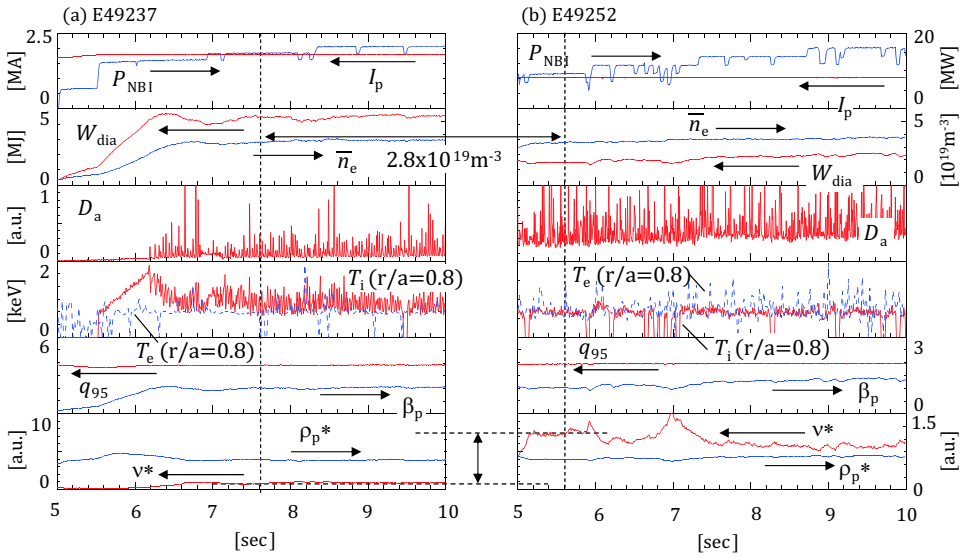

FIG. 1: Temporal evolutions of plasma parameters in H-mode discharges at (a) low and (b) high ν^*. The ρ_p^* and ν^* are measures of the volume-averaged values in arbitrary unit.

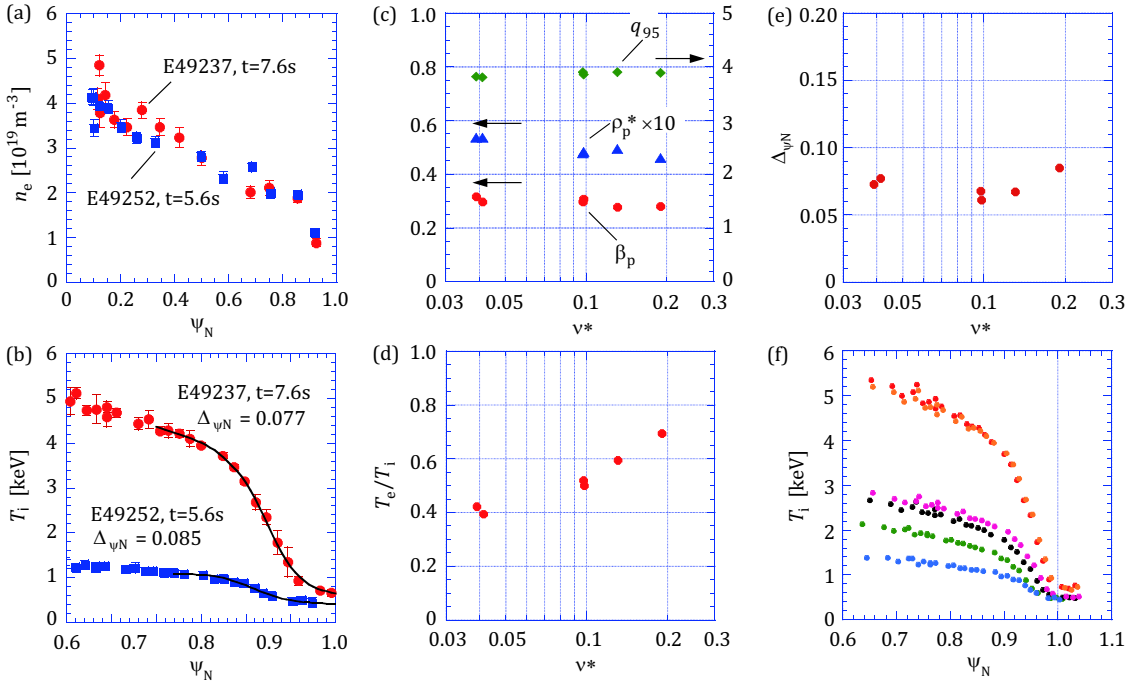

FIG. 2: Spatial profiles of (a) n_e and (b) T_i for low ν^* ($= 0.04$) and high ν^* ($= 0.19$) cases. The variations of (c) q_{95}, ρ_p^*, β_p and (d) T_e/T_i at the pedestal as a function of ν^*. (e) Dependence of the pedestal width $\Delta_{\psi N}$ on ν^*. (f) The pedestal T_i profiles in the variation of ν^*.

the expected value of the factor of $(1.79/1.03)^2 \simeq 3$ because T should scale as I_p^2. Fig. 2(c) shows the variation of q_{95}, ρ_p^* and β_p at the pedestal as a function of ν^*. The ν^* scan with the variation of $I_p = 1.03 - 1.79$MA ($B_t = 2.3 - 4.0$T) enabled us to fix q_{95}, ρ_p^* and β_p at the pedestal. Fig. 2(d) shows the variation of T_e/T_i at the pedestal as a function of ν^*. The electron-ion decoupling is enhanced at lower ν^* because ions are predominantly heated by the NBIs with the acceleration energy of ~ 85keV. This decoupling causes the difference in T_i which is larger than predicted.

Fig. 2(e) shows the dependence of the pedestal width $\Delta_{\psi N}$ on ν^*. The pedestal widths

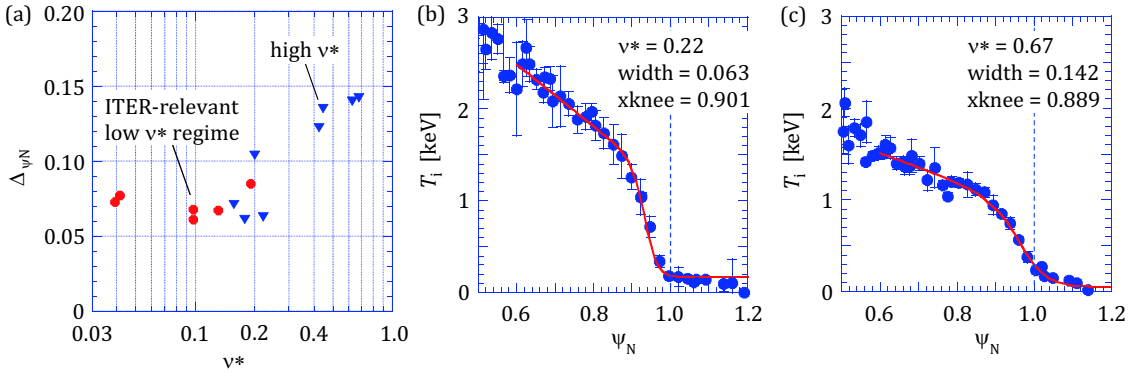

FIG. 3: (a) Dependence of the pedestal width $\Delta_{\psi N}$ on ν^*. The pedestal T_i profiles at ν^* of (b) 0.22 and (c) 0.67 in high ν^* regime.

have been evaluated by a fit with `mtanh` function. In the range of ν^* from 0.04 to 0.19, the pedestal width does not change against the variation in ν^*. Fig. 2(f) shows the pedestal T_i profiles in this ν^* scan. The experimental result indicates that the pedestal width is independent of ν^* in the ITER-relevant low ν^* regime.

3. Experiments in high ν^* regime

In high ν^* regime, ν^* was varied from 0.16 to 0.67 by deuterium gas puff rate. In this sense, this experiment is not a pure ν^* scan like the one performed in the low ν^* regime. The main aim of this study is to identify whether the pedestal width is determined only by $\beta_p^{0.5}$. As long as the pedestal β_p and magnetic geometry are fixed, the deuterium gas puff scan can be a good dataset with the variation in ν^* to see the pedestal structure other than the effect of β_p. The experiment was conducted at 1.2 MA and 2.5 T ($q_{95} \sim 3.4$) [5]. The plasma configuration is fixed at $R = 3.4$m, $a = 0.8$m, $\delta = 0.36$, $\kappa = 1.4$. The $\bar{n}_e$ is varied by gas puff from 2.4 to 3.4×10^{19}m^{-3}.

Fig. 3(a) shows the dependence of the pedestal width $\Delta_{\psi N}$ on ν^* for both scans in the low and high ν^* regime. Note that the $\Delta_{\psi N}$ values cannot simply be compared between two scans because the experimental conditions are different. In contrast to the low ν^* regime, the pedestal width becomes greater with increased ν^* in the high ν^* regime. Figs. 3(b) and (c) show the pedestal T_i profiles at low $\nu^*(= 0.22)$ and high $\nu^*(= 0.67)$, respectively. The pedestal broadening in the high ν^* regime indicates that the pedestal width cannot simply be explained by $\beta_p^{0.5}$ at the pedestal.

4. Pedestal stability analysis

Figs. 4(a) and (b) show the pedestal $j - \alpha$ diagrams in the ITER-relevant low ν^* regime. In the low ν^* regime, the pedestal is close to the peeling-ballooning mode boundary at intermediate n toroidal mode number. The most unstable mode numbers are $n = 10$ and 16 at ν^* of 0.04 and 0.19, respectively. A larger j_{bs} of ~ 0.7MA/m^2 is obtained in the low ν^* case whereas j_{bs} is ~ 0.3MA/m^2 in the high ν^* case. The pressure gradient in the steep gradient region is not significantly changed with the variation of the edge current when the pedestal stays along the peeling-ballooning boundary with the intermediate n toroidal mode number.

Figs. 4(c) and (d) show the pedestal $j - \alpha$ diagrams in the high ν^* regime. In the high ν^* regime, the pedestal is close to high n ballooning mode boundary. The most unstable

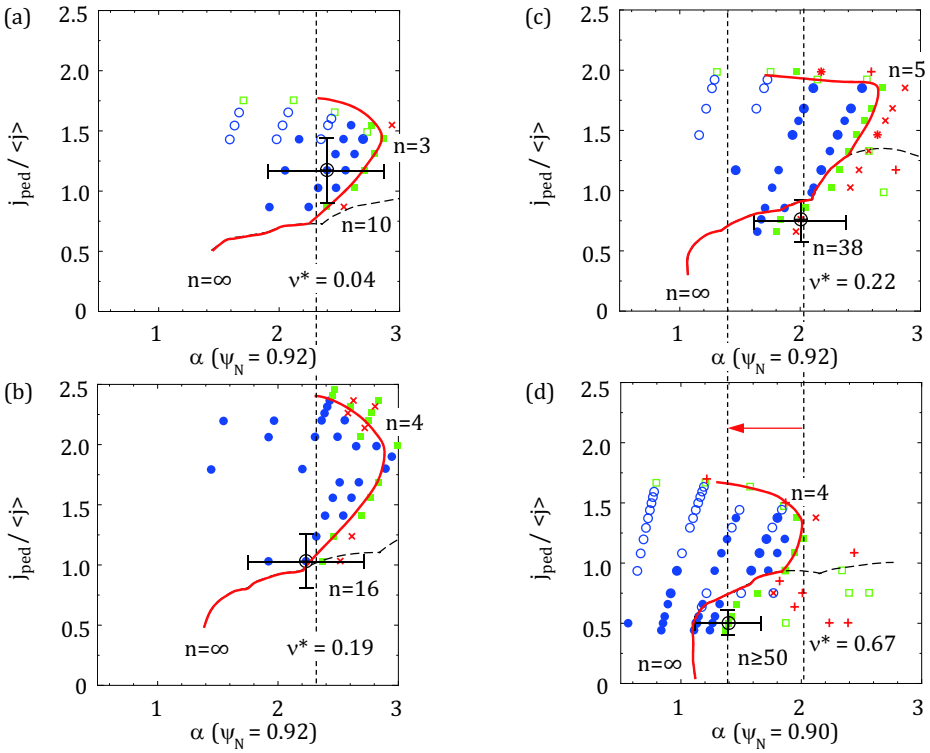

FIG. 4: The pedestal $j - \alpha$ diagrams for the ITER-relevant low ν^* scan at (a) ν^* of 0.04 and (b) 0.19 and for the high ν^* scan at (c) ν^* of 0.22 and (d) 0.67.

mode numbers are $n = 38$ and ≥ 50 at ν^* of 0.22 and 0.67, respectively. When the pedestal is destabilised by high n ballooning mode, the α decreases significantly from 2.0 to 1.3 at the steepest gradient position (or from 2.0 to 1.2 at $\psi_N = 0.92$) with the reduction in the edge current. The reduction in the pressure gradient at fixed pedestal pressure is consistent with the observation of the broadening of the pedestal width.

5. Conclusions

Dependence of pedestal width on collisionality has been investigated in JT-60U. In the ITER-relevant low ν^* regime of $0.04 < \nu^* < 0.2$, the pedestal width does not change in the variation of ν^*. In the high ν^* regime of $0.2 < \nu^* < 0.7$, the pedestal width broadens with increased ν^*. The pedestal pressure gradient is not significantly changed with the variation of the edge current at low ν^* whereas the pressure gradient decreases with the reduction in the edge current. The pedestal broadening is observed when the pedestal is unstable at high n ballooning mode. The experimental observation brings us a hypothesis that at fixed $dp/d\psi$ the pedestal can be destabilised by broadening the pedestal width to increase the edge current large enough to destabilise the peeling-ballooning mode. The analysis during the inter-ELM phase will help proving this hypothesis in the future issue.

References

[1] Urano, H., et al., Nucl. Fusion **48** (2008) 045008.
[2] Beurskens, M., et al., Phys. Plasmas **18** (2011) 056120.
[3] Kirk, A., et al., Plasma Phys. Control. Fusion **51** (2009) 065016.
[4] Walk, J.R., et al., Nucl. Fusion **52** (2012) 063011.
[5] Urano, H., et al., Nucl. Fusion **55** (2015) 033010.